

Search for the $B^+ \rightarrow K^+ \nu \bar{\nu}$ Decay Using Semi-Leptonic Tags

B. Aubert, Y. Karyotakis, J. P. Lees, V. Poireau, E. Prencipe, X. Prudent, and V. Tisserand
*Laboratoire d'Annecy-le-Vieux de Physique des Particules (LAPP),
Université de Savoie, CNRS/IN2P3, F-74941 Annecy-Le-Vieux, France*

J. Garra Tico and E. Grauges
Universitat de Barcelona, Facultat de Fisica, Departament ECM, E-08028 Barcelona, Spain

M. Martinelli^{ab}, A. Palano^{ab}, and M. Pappagallo^{ab}
INFN Sezione di Bari^a; Dipartimento di Fisica, Università di Bari^b, I-70126 Bari, Italy

G. Eigen, B. Stugu, and L. Sun
University of Bergen, Institute of Physics, N-5007 Bergen, Norway

M. Battaglia, D. N. Brown, B. Hooberman, L. T. Kerth, Yu. G. Kolomensky,
G. Lynch, I. L. Osipenkov, K. Tackmann, and T. Tanabe
Lawrence Berkeley National Laboratory and University of California, Berkeley, California 94720, USA

C. M. Hawkes, N. Soni, and A. T. Watson
University of Birmingham, Birmingham, B15 2TT, United Kingdom

H. Koch and T. Schroeder
Ruhr Universität Bochum, Institut für Experimentalphysik 1, D-44780 Bochum, Germany

D. J. Asgeirsson, C. Hearty, T. S. Mattison, and J. A. McKenna
University of British Columbia, Vancouver, British Columbia, Canada V6T 1Z1

M. Barrett, A. Khan, and A. Randle-Conde
Brunel University, Uxbridge, Middlesex UB8 3PH, United Kingdom

V. E. Blinov, A. D. Bukin,* A. R. Buzykaev, V. P. Druzhinin, V. B. Golubev,
A. P. Onuchin, S. I. Serednyakov, Yu. I. Skovpen, E. P. Solodov, and K. Yu. Todyshev
Budker Institute of Nuclear Physics, Novosibirsk 630090, Russia

M. Bondioli, S. Curry, I. Eschrich, D. Kirkby, A. J. Lankford, P. Lund, M. Mandelkern, E. C. Martin, and D. P. Stoker
University of California at Irvine, Irvine, California 92697, USA

H. Atmacan, J. W. Gary, F. Liu, O. Long, G. M. Vitug, and Z. Yasin
University of California at Riverside, Riverside, California 92521, USA

V. Sharma
University of California at San Diego, La Jolla, California 92093, USA

C. Campagnari, T. M. Hong, D. Kovalskyi, M. A. Mazur, and J. D. Richman
University of California at Santa Barbara, Santa Barbara, California 93106, USA

T. W. Beck, A. M. Eisner, C. A. Heusch, J. Kroseberg, W. S. Lockman,
A. J. Martinez, T. Schalk, B. A. Schumm, A. Seiden, L. Wang, and L. O. Winstrom
University of California at Santa Cruz, Institute for Particle Physics, Santa Cruz, California 95064, USA

C. H. Cheng, D. A. Doll, B. Echenard, F. Fang, D. G. Hitlin,

I. Narsky, P. Ongmongkolkul, T. Piatenko, and F. C. Porter
California Institute of Technology, Pasadena, California 91125, USA

R. Andreassen, G. Mancinelli, B. T. Meadows, K. Mishra, and M. D. Sokoloff
University of Cincinnati, Cincinnati, Ohio 45221, USA

P. C. Bloom, W. T. Ford, A. Gaz, J. F. Hirschauer, M. Nagel, U. Nauenberg, J. G. Smith, and S. R. Wagner
University of Colorado, Boulder, Colorado 80309, USA

R. Ayad,[†] W. H. Toki, and R. J. Wilson
Colorado State University, Fort Collins, Colorado 80523, USA

E. Feltresi, A. Hauke, H. Jasper, T. M. Karbach, J. Merkel, A. Petzold, B. Spaan, and K. Wacker
Technische Universität Dortmund, Fakultät Physik, D-44221 Dortmund, Germany

M. J. Kobel, R. Nogowski, K. R. Schubert, and R. Schwierz
Technische Universität Dresden, Institut für Kern- und Teilchenphysik, D-01062 Dresden, Germany

D. Bernard, E. Latour, and M. Verderi
Laboratoire Leprince-Ringuet, CNRS/IN2P3, Ecole Polytechnique, F-91128 Palaiseau, France

P. J. Clark, S. Playfer, and J. E. Watson
University of Edinburgh, Edinburgh EH9 3JZ, United Kingdom

M. Andreotti^{ab}, D. Bettoni^a, C. Bozzi^a, R. Calabrese^{ab}, A. Cecchi^{ab}, G. Cibirnetto^{ab}, E. Fioravanti^{ab},
P. Franchini^{ab}, E. Luppi^{ab}, M. Menerato^{ab}, M. Negrini^{ab}, A. Petrella^{ab}, L. Piemontese^a, and V. Santoro^{ab}
INFN Sezione di Ferrara^a; Dipartimento di Fisica, Università di Ferrara^b, I-44100 Ferrara, Italy

R. Baldini-Ferrolì, A. Calcaterra, R. de Sangro, G. Finocchiaro,
S. Pacetti, P. Patteri, I. M. Peruzzi,[‡] M. Piccolo, M. Rama, and A. Zallo
INFN Laboratori Nazionali di Frascati, I-00044 Frascati, Italy

R. Contri^{ab}, E. Guido, M. Lo Vetere^{ab}, M. R. Monge^{ab}, S. Passaggio^a, C. Patrignani^{ab}, E. Robutti^a, and S. Tosi^{ab}
INFN Sezione di Genova^a; Dipartimento di Fisica, Università di Genova^b, I-16146 Genova, Italy

K. S. Chaisanguanthum and M. Morii
Harvard University, Cambridge, Massachusetts 02138, USA

A. Adametz, J. Marks, S. Schenk, and U. Uwer
Universität Heidelberg, Physikalisches Institut, Philosophenweg 12, D-69120 Heidelberg, Germany

F. U. Bernlochner, V. Klose, H. M. Lacker, T. Lueck, and A. Volk
Humboldt-Universität zu Berlin, Institut für Physik, Newtonstr. 15, D-12489 Berlin, Germany

D. J. Bard, P. D. Dauncey, and M. Tibbetts
Imperial College London, London, SW7 2AZ, United Kingdom

P. K. Behera, M. J. Charles, and U. Mallik
University of Iowa, Iowa City, Iowa 52242, USA

J. Cochran, H. B. Crawley, L. Dong, V. Eyges, W. T. Meyer, S. Prell, E. I. Rosenberg, and A. E. Rubin
Iowa State University, Ames, Iowa 50011-3160, USA

Y. Y. Gao, A. V. Gritsan, and Z. J. Guo
Johns Hopkins University, Baltimore, Maryland 21218, USA

N. Arnaud, J. Béquilleux, A. D’Orazio, M. Davier, D. Derkach, J. Firmino da Costa,
G. Grosdidier, F. Le Diberder, V. Lepeltier, A. M. Lutz, B. Malaescu, S. Pruvot,

P. Roudeau, M. H. Schune, J. Serrano, V. Sordini,[§] A. Stocchi, and G. Wormser
*Laboratoire de l'Accélérateur Linéaire, IN2P3/CNRS et Université Paris-Sud 11,
 Centre Scientifique d'Orsay, B. P. 34, F-91898 Orsay Cedex, France*

D. J. Lange and D. M. Wright
Lawrence Livermore National Laboratory, Livermore, California 94550, USA

I. Bingham, J. P. Burke, C. A. Chavez, J. R. Fry, E. Gabathuler,
 R. Gamet, D. E. Hutchcroft, D. J. Payne, and C. Touramanis
University of Liverpool, Liverpool L69 7ZE, United Kingdom

A. J. Bevan, C. K. Clarke, F. Di Lodovico, R. Sacco, and M. Sigamani
Queen Mary, University of London, London, E1 4NS, United Kingdom

G. Cowan, S. Paramesvaran, and A. C. Wren
University of London, Royal Holloway and Bedford New College, Egham, Surrey TW20 0EX, United Kingdom

D. N. Brown and C. L. Davis
University of Louisville, Louisville, Kentucky 40292, USA

A. G. Denig, M. Fritsch, W. Gradl, and A. Hafner
Johannes Gutenberg-Universität Mainz, Institut für Kernphysik, D-55099 Mainz, Germany

K. E. Alwyn, D. Bailey, R. J. Barlow, G. Jackson, G. D. Lafferty, T. J. West, and J. I. Yi
University of Manchester, Manchester M13 9PL, United Kingdom

J. Anderson, C. Chen, A. Jawahery, D. A. Roberts, G. Simi, and J. M. Tuggle
University of Maryland, College Park, Maryland 20742, USA

C. Dallapiccola and E. Salvati
University of Massachusetts, Amherst, Massachusetts 01003, USA

R. Cowan, D. Dujmic, P. H. Fisher, S. W. Henderson, G. Sciolla, M. Spitznagel, R. K. Yamamoto, and M. Zhao
Massachusetts Institute of Technology, Laboratory for Nuclear Science, Cambridge, Massachusetts 02139, USA

P. M. Patel, S. H. Robertson, and M. Schram
McGill University, Montréal, Québec, Canada H3A 2T8

P. Biassoni^{ab}, A. Lazzaro^{ab}, V. Lombardo^a, F. Palombo^{ab}, and S. Stracka^{ab}
INFN Sezione di Milano^a; Dipartimento di Fisica, Università di Milano^b, I-20133 Milano, Italy

L. Cremaldi, R. Godang,[¶] R. Kroeger, P. Sonnek, D. J. Summers, and H. W. Zhao
University of Mississippi, University, Mississippi 38677, USA

M. Simard and P. Taras
Université de Montréal, Physique des Particules, Montréal, Québec, Canada H3C 3J7

H. Nicholson
Mount Holyoke College, South Hadley, Massachusetts 01075, USA

G. De Nardo^{ab}, L. Lista^a, D. Monorchio^{ab}, G. Onorato^{ab}, and C. Sciacca^{ab}
*INFN Sezione di Napoli^a; Dipartimento di Scienze Fisiche,
 Università di Napoli Federico II^b, I-80126 Napoli, Italy*

G. Raven and H. L. Snoek
NIKHEF, National Institute for Nuclear Physics and High Energy Physics, NL-1009 DB Amsterdam, The Netherlands

C. P. Jessop, K. J. Knoepfel, J. M. LoSecco, and W. F. Wang

University of Notre Dame, Notre Dame, Indiana 46556, USA

L. A. Corwin, K. Honscheid, H. Kagan, R. Kass, J. P. Morris, A. M. Rahimi, S. J. Sekula, and Q. K. Wong
Ohio State University, Columbus, Ohio 43210, USA

N. L. Blount, J. Brau, R. Frey, O. Igonkina, J. A. Kolb, M. Lu,
R. Rahmat, N. B. Sinev, D. Strom, J. Strube, and E. Torrence
University of Oregon, Eugene, Oregon 97403, USA

G. Castelli^{ab}, N. Gagliardi^{ab}, M. Margoni^{ab}, M. Morandin^a,
M. Posocco^a, M. Rotondo^a, F. Simonetto^{ab}, R. Stroili^{ab}, and C. Voci^{ab}
INFN Sezione di Padova^a; Dipartimento di Fisica, Università di Padova^b, I-35131 Padova, Italy

P. del Amo Sanchez, E. Ben-Haim, G. R. Bonneaud, H. Briand, J. Chauveau,
O. Hamon, Ph. Leruste, G. Marchiori, J. Ocariz, A. Perez, J. Prendki, and S. Sitt
*Laboratoire de Physique Nucléaire et de Hautes Energies,
IN2P3/CNRS, Université Pierre et Marie Curie-Paris6,
Université Denis Diderot-Paris7, F-75252 Paris, France*

L. Gladney
University of Pennsylvania, Philadelphia, Pennsylvania 19104, USA

M. Biasini^{ab} and E. Manoni^{ab}
INFN Sezione di Perugia^a; Dipartimento di Fisica, Università di Perugia^b, I-06100 Perugia, Italy

C. Angelini^{ab}, G. Batignani^{ab}, S. Bettarini^{ab}, G. Calderini^{ab},** M. Carpinelli^{ab},†† A. Cervelli^{ab}, F. Forti^{ab},
M. A. Giorgi^{ab}, A. Lusiani^{ac}, M. Morganti^{ab}, N. Neri^{ab}, E. Paoloni^{ab}, G. Rizzo^{ab}, and J. J. Walsh^a
INFN Sezione di Pisa^a; Dipartimento di Fisica, Università di Pisa^b; Scuola Normale Superiore di Pisa^c, I-56127 Pisa, Italy

D. Lopes Pegna, C. Lu, J. Olsen, A. J. S. Smith, and A. V. Telnov
Princeton University, Princeton, New Jersey 08544, USA

F. Anulli^a, E. Baracchini^{ab}, G. Cavoto^a, R. Faccini^{ab}, F. Ferrarotto^a, F. Ferroni^{ab}, M. Gaspero^{ab},
P. D. Jackson^a, L. Li Gioi^a, M. A. Mazzoni^a, S. Morganti^a, G. Piredda^a, F. Renga^{ab}, and C. Voena^a
*INFN Sezione di Roma^a; Dipartimento di Fisica,
Università di Roma La Sapienza^b, I-00185 Roma, Italy*

M. Ebert, T. Hartmann, H. Schröder, and R. Waldi
Universität Rostock, D-18051 Rostock, Germany

T. Adye, B. Franek, E. O. Olaiya, and F. F. Wilson
Rutherford Appleton Laboratory, Chilton, Didcot, Oxon, OX11 0QX, United Kingdom

S. Emery, L. Esteve, G. Hamel de Monchenault, W. Kozanecki, G. Vasseur, Ch. Yèche, and M. Zito
CEA, Irfu, SPP, Centre de Saclay, F-91191 Gif-sur-Yvette, France

M. T. Allen, D. Aston, R. Bartoldus, J. F. Benitez, R. Cenci, J. P. Coleman, M. R. Convery, J. C. Dingfelder,
J. Dorfan, G. P. Dubois-Felsmann, W. Dunwoodie, R. C. Field, M. Franco Sevilla, B. G. Fulsom,
A. M. Gabareen, M. T. Graham, P. Grenier, C. Hast, W. R. Innes, J. Kaminski, M. H. Kelsey, H. Kim,
P. Kim, M. L. Kocian, D. W. G. S. Leith, S. Li, B. Lindquist, S. Luitz, V. Luth, H. L. Lynch,
D. B. MacFarlane, H. Marsiske, R. Messner,* D. R. Muller, H. Neal, S. Nelson, C. P. O'Grady, I. Ofte,
M. Perl, B. N. Ratcliff, A. Roodman, A. A. Salnikov, R. H. Schindler, J. Schwiening, A. Snyder, D. Su,
M. K. Sullivan, K. Suzuki, S. K. Swain, J. M. Thompson, J. Va'vra, A. P. Wagner, M. Weaver, C. A. West,
W. J. Wisniewski, M. Wittgen, D. H. Wright, H. W. Wulsin, A. K. Yarritu, C. C. Young, and V. Ziegler
SLAC National Accelerator Laboratory, Stanford, California 94309 USA

X. R. Chen, H. Liu, W. Park, M. V. Purohit, R. M. White, and J. R. Wilson

University of South Carolina, Columbia, South Carolina 29208, USA

M. Bellis, P. R. Burchat, A. J. Edwards, and T. S. Miyashita
Stanford University, Stanford, California 94305-4060, USA

S. Ahmed, M. S. Alam, J. A. Ernst, B. Pan, M. A. Saeed, and S. B. Zain
State University of New York, Albany, New York 12222, USA

A. Soffer
Tel Aviv University, School of Physics and Astronomy, Tel Aviv, 69978, Israel

S. M. Spanier and B. J. Wogslund
University of Tennessee, Knoxville, Tennessee 37996, USA

R. Eckmann, J. L. Ritchie, A. M. Ruland, C. J. Schilling, R. F. Schwitters, and B. C. Wray
University of Texas at Austin, Austin, Texas 78712, USA

B. W. Drummond, J. M. Izen, and X. C. Lou
University of Texas at Dallas, Richardson, Texas 75083, USA

F. Bianchi^{ab}, D. Gamba^{ab}, and M. Pelliccioni^{ab}
INFN Sezione di Torino^a; Dipartimento di Fisica Sperimentale, Università di Torino^b, I-10125 Torino, Italy

M. Bomben^{ab}, L. Bosisio^{ab}, C. Cartaro^{ab}, G. Della Ricca^{ab}, L. Lanceri^{ab}, and L. Vitale^{ab}
INFN Sezione di Trieste^a; Dipartimento di Fisica, Università di Trieste^b, I-34127 Trieste, Italy

V. Azzolini, N. Lopez-March, F. Martinez-Vidal, D. A. Milanese, and A. Oyanguren
IFIC, Universitat de Valencia-CSIC, E-46071 Valencia, Spain

J. Albert, Sw. Banerjee, B. Bhuyan, H. H. F. Choi, K. Hamano, G. J. King,
R. Kowalewski, M. J. Lewczuk, I. M. Nugent, J. M. Roney, and R. J. Sobie
University of Victoria, Victoria, British Columbia, Canada V8W 3P6

T. J. Gershon, P. F. Harrison, J. Ilic, T. E. Latham, G. B. Mohanty, and E. M. T. Puccio
Department of Physics, University of Warwick, Coventry CV4 7AL, United Kingdom

H. R. Band, X. Chen, S. Dasu, K. T. Flood, Y. Pan, R. Prepost, C. O. Vuosalo, and S. L. Wu
University of Wisconsin, Madison, Wisconsin 53706, USA

(Dated: April 30, 2022)

We present an update of the search for the flavor-changing neutral current $B^+ \rightarrow K^+ \nu \bar{\nu}$ decay using 351×10^6 $B\bar{B}$ pairs collected at the $\Upsilon(4S)$ resonance with the BABAR detector at the SLAC PEP-II B factory. Due to the presence of two neutrinos in the final state, we require the reconstruction of the companion B in the event through the decay channel $B^- \rightarrow D^0 \ell^- \bar{\nu} X$. We find 38 candidates in the data with an expected background of 31 ± 12 . This allows us to set an upper limit on the branching fraction for $B^+ \rightarrow K^+ \nu \bar{\nu}$ of 4.5×10^{-5} at 90% confidence level.

PACS numbers: 13.25.Hw, 12.15.Hh, 11.30.Er

*Deceased

†Now at Temple University, Philadelphia, Pennsylvania 19122, USA

‡Also with Università di Perugia, Dipartimento di Fisica, Perugia, Italy

§Also with Università di Roma La Sapienza, I-00185 Roma, Italy

¶Now at University of South Alabama, Mobile, Alabama 36688, USA

**Also with Laboratoire de Physique Nucléaire et de Hautes Energies, IN2P3/CNRS, Université Pierre et Marie Curie-Paris6, Université Denis Diderot-Paris7, F-75252 Paris, France

††Also with Università di Sassari, Sassari, Italy

I. INTRODUCTION

Flavor-changing neutral-current transitions such as $b \rightarrow s\nu\bar{\nu}$ are absent at tree level in the Standard Model (SM) and occur only via electroweak penguin diagrams or one-loop box diagrams with virtual heavy particles in the loops, as shown in Fig. 1. Because such loop production processes are generally suppressed, the SM predicts $b \rightarrow s\nu\bar{\nu}$ transitions to be very rare. We report herein the results of a search for the exclusive decay mode $B^+ \rightarrow K^+\nu\bar{\nu}$ (charge conjugation is implied throughout this paper). The SM prediction of the branching fraction is $\mathcal{B}(B^+ \rightarrow K^+\nu\bar{\nu}) = (3.8_{-0.6}^{+1.2}) \times 10^{-6}$ [1], and the most stringent published upper limit at 90% confidence level is $\mathcal{B}(B^+ \rightarrow K^+\nu\bar{\nu}) < 1.4 \times 10^{-5}$ [2] by the Belle Collaboration with $535 \times 10^6 B\bar{B}$ pairs. This analysis serves as an independent measurement of the limit on this branching fraction.

With current luminosity, we do not have the sensitivity to measure a branching fraction at the level of the SM; however several new physics models may increase the rate of $b \rightarrow s\nu\bar{\nu}$ transitions. The Minimal Supersymmetric Standard Model with large $\tan\beta$ [3] leads to higher rates through chargino and/or charged Higgs contributions to the loop diagram. “Unparticle models” [4] can give an observed enhancement because of the similarities in decay signatures between a $B^+ \rightarrow K^+\nu\bar{\nu}$ decay and a decay containing an unparticle. Models with a single universal extra dimension [5] enhance the observed rate at lower values of $1/R$, where R is the compactification radius of the extra dimension. Also, models with light scalar dark matter candidates having GeV/c^2 or sub- GeV/c^2 masses [6] may increase the observed rate because of the similarity in decay signatures between $B^+ \rightarrow K^+\nu\bar{\nu}$ and a decay containing two dark matter scalars.

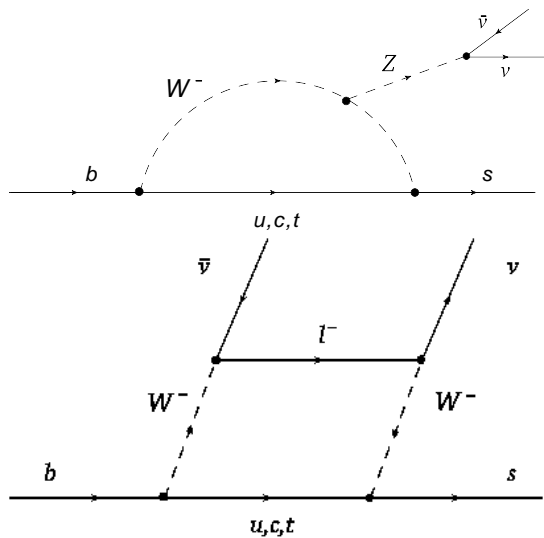


FIG. 1: The $b \rightarrow s\nu\bar{\nu}$ transition proceeding through a penguin diagram (top) and a box diagram (bottom).

Due to the presence of multiple neutrinos, the $B^+ \rightarrow K^+\nu\bar{\nu}$ decay mode lacks the kinematic constraints that are usually exploited in B decay searches at B factories to reject both continuum (non- $B\bar{B}$) and $B\bar{B}$ backgrounds. The strategy adopted for this analysis is to reconstruct an exclusive decay of the B^- meson in the event, the “tag B ,” in one of several semileptonic decay modes. All remaining charged and neutral particles in the event are examined under the assumption that they are products of the accompanying B decay, the “signal B .” We perform a multivariate analysis using a random forest classifier (explained below) to separate signal events from background events. We keep the signal region of the classifier output blind to avoid experimenter bias. The random forest classifier introduces very different systematic uncertainties than this collaboration’s previous measurement [7].

II. THE BABAR DETECTOR AND DATASET

The data used in this analysis were collected with the *BABAR* detector [8] at the PEP-II asymmetric e^+e^- storage ring. The sample corresponds to an integrated luminosity of 319fb^{-1} at the $\Upsilon(4S)$ resonance, and consists of about $351 \times 10^6 B\bar{B}$ pairs. Charged-particle tracking and dE/dx measurements for particle identification (PID) are provided by a five-layer double-sided silicon vertex tracker (SVT) and a 40-layer drift chamber (DCH) in a 1.5 T axial magnetic field. A ring imaging Cherenkov detector (DIRC) is used for $\pi - K$ discrimination. The energies of neutral particles are measured by an electromagnetic calorimeter (EMC) consisting of 6580 CsI(Tl) crystals. The magnetic flux return of the solenoid, instrumented with resistive plate chambers and limited streamer tubes, provides muon identification.

A GEANT4-based [9] Monte Carlo (MC) simulation is used to model the *BABAR* detector response, taking into account the varying accelerator and detector conditions. Dedicated signal and background MC samples are used to estimate the signal selection efficiency and determine the expected number of background events. Simulation samples are used to model $B\bar{B}$ events and continuum $e^+e^- \rightarrow u\bar{u}, d\bar{d}, s\bar{s}, c\bar{c}$, and $\tau^+\tau^-$ events (background MC events). A sample of 1.37×10^6 events is simulated in which the B^+ meson decays to $K^+\nu\bar{\nu}$, and the B^- meson decays to a mode with at least one lepton in the final state (signal MC events).

III. ANALYSIS METHOD

A. Tag B Reconstruction

The tag B reconstruction combines a D^0 meson with a single identified charged lepton to form a $D^0\ell$ candidate. The lepton candidate must have PID information consistent with an electron or a muon, have a minimum transverse momentum of $0.1\text{GeV}/c$, and have at least 20

hits in the DCH. The D^0 candidates are reconstructed in three decay modes: $K^-\pi^+$, $K^-\pi^+\pi^-\pi^+$, and $K^-\pi^+\pi^0$. The charged pions from the D^0 decay must have a polar angle between 0.41 and 2.54 radians. The K^- candidate must fail π^- PID requirements based on the candidate's measured dE/dx for lower momentum candidates, or on the Cherenkov angle, number of photons, and track quality measured in the DIRC for higher momentum candidates. The π^0 candidates are required to have a reconstructed mass between $0.115 < m_{\pi^0} < 0.150$ GeV/ c^2 , and have an energy measured in the laboratory frame greater than 0.2 GeV. The reconstructed D^0 mass, m_{D^0} , must be within 0.04 GeV/ c^2 (0.07 GeV/ c^2) of the nominal D^0 mass for the channels without (with) a π^0 in the final state, and the center of mass momentum, p_{D^0} , must be greater than 0.5 GeV/ c . The invariant mass, $m_{D^0\ell}$, of the $D^0\ell$ candidate must be greater than 3.0 GeV/ c^2 .

Assuming that a neutrino is the only particle missing from a genuine $B^- \rightarrow D^0\ell^-\bar{\nu}$ decay, the cosine of the angle between the direction of the reconstructed tag B and that of the $D^0\ell$ candidate, described by the four vector $(E_{D^0\ell}, \mathbf{p}_{D^0\ell})$, is given by

$$\cos\theta_{B,D^0\ell} = \frac{2E_B E_{D^0\ell} - m_B^2 - m_{D^0\ell}^2}{2|p_{D^0\ell}|\sqrt{E_B^2 - m_B^2}}, \quad (1)$$

where m_B is the nominal B meson mass and E_B and $\sqrt{E_B^2 - m_B^2}$ are the expected B meson energy and momentum, respectively, fixed by the energies of the beams and evaluated in the center of mass frame. We retain events in the interval $-2.5 < \cos\theta_{B,D^0\ell} < 1.1$. These bounds are outside the allowed physical region to maintain efficiency for $B^- \rightarrow D^{*0}\ell^-\bar{\nu}$ decays in which a π^0 or photon has not been reconstructed as part of the $D^0\ell$ combination and to account for resolution effects. If more than one $D^0\ell$ candidate is reconstructed in a given event, the one with the smallest $|\cos\theta_{B,D^0\ell}|$ is retained. The m_{D^0} distribution remains unbiased by this method of choosing the best candidate, allowing us to later use it for background estimations (SEC. III C).

B. Signal Event Selection

Events containing a reconstructed tag B are examined for evidence of a $B^+ \rightarrow K^+\nu\bar{\nu}$ decay. We require that the number of charged tracks remaining after the tag B has been reconstructed is less than 4, and that the missing energy in the event is greater than 2.5 GeV. The signal K^+ candidate must satisfy PID criteria, have a polar angle between 0.469 and 2.457 radians (the angular acceptance of the DIRC), and have a charge opposite that of the lepton in the tagged B decay. After applying these preliminary requirements, the MC samples are reweighted to reproduce the selection efficiencies determined on the data. We use a bagged decision tree multivariate classifier (random forest classifier [10]), available in the StatPattern-Recognition software package [11], to discriminate signal

events from background. This method, a powerful alternative to “rectangular cuts,” separates events of different categories by training many decision trees (sequential partitioning of data into subsets of similar characteristics starting from a root node) [12]. We choose to use a random forest classifier instead of another multivariate classifier because of its stability with higher dimensionality (more input variables), its training stability (the performance is less likely to diminish with continued training), and its insensitivity to input variables with weak discriminating power.

We use the 19 variables listed in Table I in the classifier, the most important of which are the number of charged tracks not used in the tag B reconstruction, the total energy of signal side photons each with energy greater than 0.05 GeV (lower energy photons are not modeled as well in our MC events), the signal-kaon momentum, and the missing energy of the event. Distributions of these variables (Fig. 2) show a clear difference between signal events and the different types of background.

To avoid overtraining of the classifier, we separate the MC events equally between two samples. The classifier is trained on one sample, while the other is used to determine if the classifier is overtrained and what the signal and background efficiencies are when cutting on the classifier output. We train the classifier by optimizing the Punzi figure of merit (FOM) [13]

$$\frac{N_S}{0.5 \cdot N_\sigma + \sqrt{N_B}}, \quad (2)$$

where N_S is the expected number of signal events (assuming the SM branching fraction), N_B is the number of expected background events, and N_σ is the sigma level of significance, taken here to be 3. The output of the random forest classifier is shown in Fig. 3 for MC simulated signal and background events. Based on MC predictions, the multivariate classifier improves the FOM by 34% over rectangular selection requirements.

We define the signal region by requiring the output of the multivariate classifier be greater than 0.82. This selection is optimized using signal and background MC samples to maximize the FOM given in Eq. 2. When combined with the efficiency of reconstructing the tag B , this gives a total signal efficiency of $\epsilon = (0.16 \pm 0.02)\%$. The quoted error is the quadratic sum of the statistical, theoretical, and systematic uncertainties; we discuss the latter two below.

C. Background Estimation

We divide the distribution of the invariant mass of the D^0 candidate into a high and low sideband and a signal region, defined in Table II. This variable shows no correlation with the output of the random forest. We identify two types of background in our signal region: combinatoric backgrounds, which are linear in the m_{D^0} distribution shown in Fig. 4, and peaking backgrounds, which

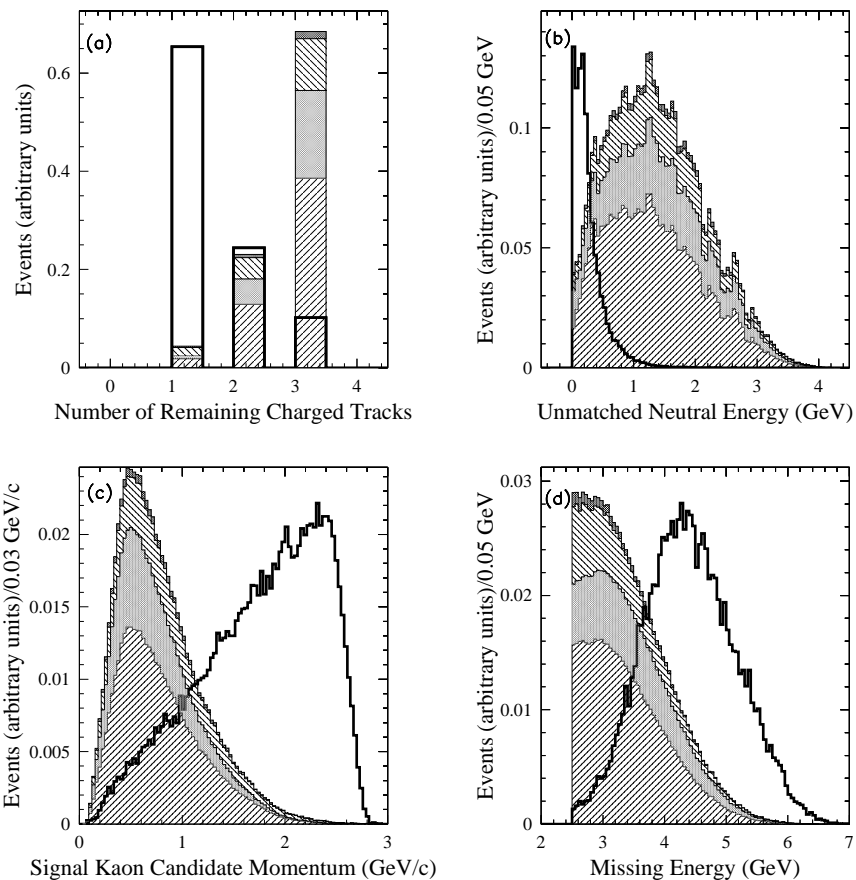


FIG. 2: Several important variables that are used in the random forest classifier. (a) The number of charged tracks in the event not used for tag B reconstruction, (b) the total energy of photons ($E_\gamma > 0.05$ GeV) not used in the tag B reconstruction, (c) the momentum of the signal B kaon candidate, and (d) the missing energy. These are shown for the signal MC events (bold black-outlined histogram) and the different types of background; starting from the bottom of the stacked histogram, these are B^+B^- (hatched), $B^0\bar{B}^0$ (light grey), $c\bar{c}$ (hatched), and $u\bar{u}$, $s\bar{s}$, $d\bar{d}$ (black). The signal MC distribution has been normalized to unit area and the background classes have been normalized by an arbitrary constant, but reflect the relative amounts of each class as expected in the data.

correspond to true D^0 candidates and peak in the m_{D^0} distribution. The combinatoric background level is estimated from the number of events in the m_{D^0} sidebands that pass all cuts. The level of combinatoric background expected in the signal region is 22 ± 5 events, where the uncertainty is statistical.

To evaluate the peaking backgrounds, we start with the random forest output of events in the m_{D^0} signal region after subtracting the non-peaking part using the m_{D^0} sidebands. This distribution is produced for both MC and data and their ratio is shown in Fig. 5. We fit a line to the points in which the output of the classifier is less than 0.82 (the background region) and extrapolate it into the signal region. The slope of the line is different from 0 and yields a multiplicative correction of 1.29 to the peaking component of our MC sample in the signal region that accounts for discrepancies between data and simulated events. The level of peaking background expected in the

signal region is 9 ± 10 events, where the uncertainty is statistical.

IV. SYSTEMATIC UNCERTAINTY STUDIES

We vary the functions used to determine the estimated number of combinatoric and peaking background events in order to obtain the associated systematic uncertainties. This yields a systematic uncertainty of ± 1.9 events for the combinatoric background estimate and ± 3.2 events for the peaking background estimate. We associate an uncertainty with reweighting the MC samples after the preliminary requirements (± 3.0 events), taken to be the difference between the number of events expected with and without this reweighting.

The systematic uncertainty associated with the requirement on the output of the random forest classifier

TABLE I: Descriptions of the variables input to the random forest classifier.

Tag B Variables	
1.	Number of charged tracks used to reconstruct the B
2.	Number of π^0 's in the D^0 decay mode
3.	The cosine of the angle between the thrust axis and the z -axis in the center of mass
4.	Total momentum transverse to the z -axis
5.	Cosine of the angle of the momentum vector of the $D^0\ell$ candidate to the z -axis in the center of mass
6.	Center of mass momentum of the lepton candidate
7.	Cosine of the angle between the tag side momentum of the combined $D^0\ell$ and the momentum of the parent B meson in the center of mass
Signal B Variables	
8.	Number of charged tracks remaining after reconstruction of the tag side
9.	Total energy of photons with $E_\gamma > 50$ MeV, after the tag side reconstruction
10.	Momentum of the signal side kaon in the center of mass
11.	Number of photons with $E_\gamma > 50$ MeV, remaining after the tag side reconstruction
12.	Cosine of the angle between the signal side kaon and the tag side lepton candidate in the center of mass
13.	Cosine of the angle between the signal side kaon and the tag side D candidate in the center of mass
14.	Cosine of the angle between the signal side kaon and the tag side $D^0\ell$ candidate in the center of mass
15.	Number of π^0 candidates remaining after tag side reconstruction
Event Variables	
17.	Amount of undetected energy
18.	Amount of undetected mass
19.	2nd Fox-Wolfram moment [14]

TABLE II: The mode-specific m_{D^0} (in units of GeV/c^2) side-band definitions. The boundaries for the third mode differ from those of the first two due to the presence of a π^0 .

D^0 mode	Lower Side	Signal Region	Upper Side
$K\pi, K\pi\pi\pi$	1.8245-1.8445	1.8445-1.8845	1.8845-1.9045
$K\pi\pi^0$	1.7945-1.8295	1.8295-1.8995	1.8995-1.9345

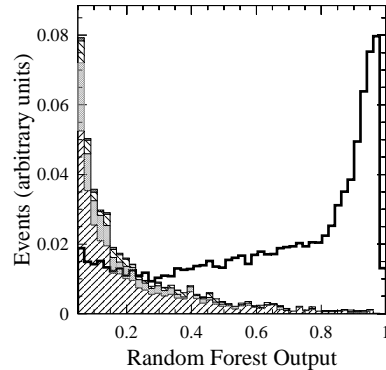


FIG. 3: The output of the random forest classifier for the signal MC events (bold black-outlined histogram) and the different types of background; starting from the bottom of the stacked histogram these are B^+B^- (hatched), $B^0\bar{B}^0$ (light grey), $c\bar{c}$ (hatched), and $u\bar{u}, s\bar{s}, d\bar{d}$ (black). The signal MC distribution has been normalized to unit area and the background classes have been normalized by an arbitrary constant, but reflect the relative amounts of each class as expected in the data.

is evaluated by selecting a double tag sample in both the data and the MC events in which both B mesons decay semileptonically. Using particle substitution on one of the two semileptonically-tagged B mesons ($D^0 \rightarrow K, l^+ \rightarrow \nu$), we model the distributions of the variables that are included in the random forest classifier to resemble the signal MC events' distributions. This second tagged B meson serves as a control sample to estimate the difference in selection efficiency between MC events and data of the random forest classifier. This difference between the double tag data and MC efficiencies (5.2%) is assigned as the systematic uncertainty for how well the MC sample models the data. An additional contribution of 9.3% accounts for the difference between our control sample (double tag MC events) and our signal MC sample. Added in quadrature, the total uncertainty due to the random forest selection is 10.7%.

Additional systematic uncertainties associated with the $B^+ \rightarrow K^+\nu\bar{\nu}$ signal efficiency include uncertainties in the tagging efficiency (6.5%), in the PID criteria used to identify the signal kaon (3.5%), and in the tracking efficiency (0.5%). We evaluate the tagging uncertainty using the double tag sample, with both D^0 's decaying to $K^-\pi^+$. We take the ratio of the efficiency of finding both tags to the efficiency of finding one tag in both the MC sample and the data. We then compare these ratios to determine the associated systematic uncertainty.

The theoretical uncertainty on the K^+ momentum spectrum in $B^+ \rightarrow K^+\nu\bar{\nu}$ decays results in a 3.1% uncertainty on the signal efficiency. This uncertainty is evaluated by comparing the efficiency obtained using the kaon momentum spectrum given in Ref. [1] and the ef-

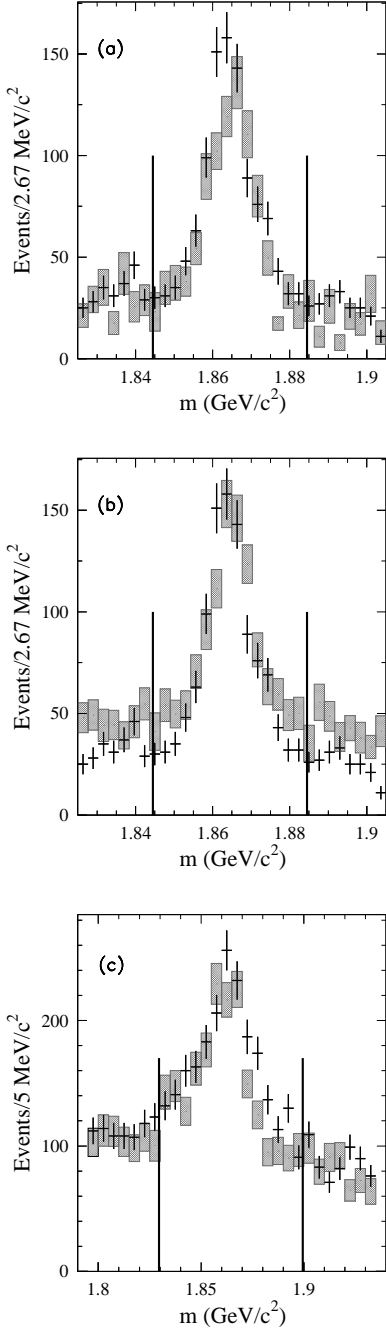


FIG. 4: A comparison of the invariant mass distributions of the D^0 candidates for the MC events and the data; the MC predictions are the grey rectangles (the height representing the uncertainty) and the data are the black points with error bars. The boundary between the signal and sideband regions is shown by the vertical black lines. Plot (a) is the $K\pi$ mode, (b) is the $K\pi\pi\pi$ mode, and (c) is the $K\pi\pi^0$ mode.

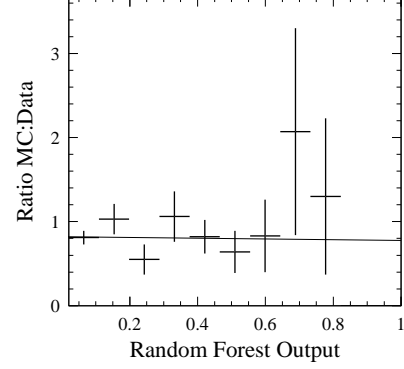


FIG. 5: The ratio of the number of MC events to the number of data events in the m_{D^0} signal region of each bin of the random forest classifier's output after background subtraction. The linear fit described in the text is also shown.

TABLE III: Systematic uncertainties on signal efficiency (in %).

Systematic Uncertainties	
Random Forest Selection	10.7
Tagging	6.5
Kaon PID	3.5
Tracking	0.5
Kaon Momentum	3.1
Total	13.4

efficiency obtained when the sample is generated using a phase space model for the decay. These theoretical and systematic uncertainties on the signal efficiency are summarized in Table III.

V. RESULTS

We expect 31 ± 12 background events in the signal region, and the SM predicts 2.2 signal events. The signal efficiency is $(0.16 \pm 0.02)\%$, which, using the Bayesian procedure described in [15], yields an expected upper limit of 3.1×10^{-5} at 90% confidence level. We observe 38 events in the signal region. The distributions of the random forest classifier's output for the data and background Monte Carlo events are shown in Fig. 6. Because the number of events we see is consistent with the expected background, we interpret these results in the context of the SM, and set an upper limit on the branching

fraction at $\mathcal{B}(B^+ \rightarrow K^+\nu\bar{\nu}) < 4.5 \times 10^{-5}$ at 90% confidence level. This is an improvement over *BABAR*'s previous search for this mode [7], which set an upper limit at $\mathcal{B}(B^+ \rightarrow K^+\nu\bar{\nu}) < 5.2 \times 10^{-5}$ using both semileptonic and hadronic tagged events, and is consistent with the recent, more stringent, limit by the Belle Collaboration [2].

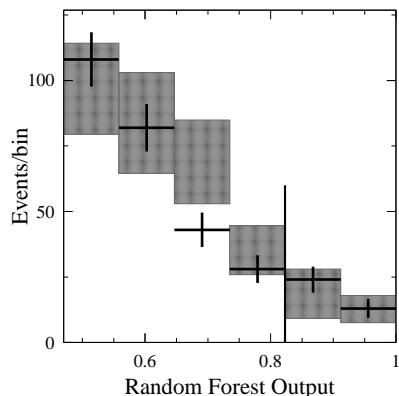


FIG. 6: The distribution of the random forest classifier's output for data (crosses). The expected range for the number of background events is shown as the grey boxes. The vertical black bar shows the cut on the random forest classifier's output: the signal region is to the right.

We are grateful for the extraordinary contributions of our PEP-II colleagues in achieving the excellent luminosity and machine conditions that have made this work possible. The success of this project also relies critically on the expertise and dedication of the computing organizations that support *BABAR*. The collaborating institutions wish to thank SLAC for its support and the kind hospitality extended to them. This work is supported by the US Department of Energy and National Science Foundation, the Natural Sciences and Engineering Research Council (Canada), the Commissariat à l'Énergie Atomique and Institut National de Physique Nucléaire et de Physique des Particules (France), the Bundesministerium für Bildung und Forschung and Deutsche Forschungsgemeinschaft (Germany), the Istituto Nazionale di Fisica Nucleare (Italy), the Foundation for Fundamental Research on Matter (The Netherlands), the Research Council of Norway, the Ministry of Education and Science of the Russian Federation, Ministerio de Educación y Ciencia (Spain), and the Science and Technology Facilities Council (United Kingdom). Individuals have received support from the Marie-Curie IEF program (European Union) and the A. P. Sloan Foundation.

-
- [1] G. Buchalla, G. Hiller, and G. Isidori, *Phys. Rev. D* **63**, 014015 (2001).
 - [2] Belle Collaboration, K. F. Chen *et al.*, *Phys. Rev. Lett.* **99**, 221802 (2007).
 - [3] Y. Yamada, *Phys. Rev. D* **77**, 014025 (2008).
 - [4] T. M. Aliev, A. S. Cornell, and N. Gaur, *JHEP* **0707**, 072 (2007).
 - [5] P. Colangelo, F. De Fazio, R. Ferrandes, and T. N. Pham, *Phys. Rev. D* **73**, 115006 (2006).
 - [6] C. Bird, P. Jackson, R. Kowalewski, and M. Pospelov, *Phys. Rev. Lett.* **93**, 201803 (2004).
 - [7] *BABAR* Collaboration, B. Aubert *et al.*, *Phys. Rev. Lett.* **94**, 101801 (2005).
 - [8] *BABAR* Collaboration, B. Aubert *et al.*, *Nucl. Instrum. Methods Phys. Res., Sect. A* **479**, 1 (2002).
 - [9] S. Agostinelli *et al.*, *Nucl. Instrum. Methods Phys. Res., Sect. A* **506**, 250 (2003).
 - [10] L. Breiman, *Machine Learning* **45**, 5 (2001).
 - [11] I. Narsky, *StatPatternRecognition*, 2009, Retrieved from <http://statpatrec.sourceforge.net/>.
 - [12] L. Breiman, *Classification and Regression Trees*, Waldsworth International Group, Belmont (1984).
 - [13] G. Punzi, *Proceedings of PHYSTAT2003: Statistical Problems in Particle Physics, Astrophysics, and Cosmology*, Menlo Park, 79 (2003).
 - [14] G. Fox, S. Wolfram, *Nucl. Phys. B* **149**, 413 (1979).
 - [15] R. Barlow, *Computer Physics Communications* **149**, 97 (2002).